by LAS-3000 (Fujifilm, Kanagawa, Japan).

GluA2 Phosphorylation in Chemical LTD. Sagittal cerebellar slices from the P21–35 mice were prepared as described above. After 1-h incubation in ACSF containing 100 μM picrotoxin, the slices were transferred to a humidified and oxygenated treatment chamber and recovered for additional 30 min. To induce chemical LTD, cerebellar slices were exposed to the K-glu solution, the ACSF supplemented with 50 mM KCl and 10 μM L-glutamate, for 5 min. After 10-min washing, the slices were immediately frozen with liquid nitrogen. To obtain the lysates, we added the lysis buffer containing 150 NaCl, 50 Tris-HCl (pH 7.5), 5 EDTA, 1 Na vanadate (in mM) and 1% SDS with protease inhibitors and serine/threonine phosphatase inhibitors and applied sonication at 4°C. The samples were boiled and centrifuged at 13,000 rpm for 15 min. An equal volume of 2 × SDS-PAGE buffer was added to the supernatant. Ten to fifteen μg of protein from each lysate was subjected to SDS-PAGE and analyzed by western blotting. To induce chemical LTD in the presence of a PP1 analog, we pretreated cerebellar slices with 50 μM PP1 analog for 30 min and included the PP1 analog throughout the LTD experiment.

GluA2 Dephosphorylation in HEK293 Cells. pTracer-GluA2 and pCAGGS-HA-PTPMEG or -HA-PTPMEG^{DA} were co-transfected to HEK293 cells by the calcium phosphate method (CellPhect; BD Biosciences). Following over-night incubation, cells were collected and treated with 2 × SDS-PAGE loading buffer. The sonicated samples were boiled for 5 min and 10 μg of extracted protein was used for

western blot analysis. Quantification of western blot was performed with MultiGauge (Fujifilm). For quantitative comparison, immunoreactivity of phosphorylated GluA2 was normalized by that of GluA2 and the ratio to the control group was calculated.

***In vitro* Phosphorylation of GST-GluA2-CT**. GST-fusion protein of the GluA2 C-terminal cytoplasmic region (GST-GluA2-CT) was prepared. Following autophosphorylation reaction of Src (Invitrogen) in the buffer containing 20 mM HEPES (pH 7.35), 3 mM $MnCl_2$ and 0.1 mM ATP at 30°C for 15 min, 0.5–1 μg of GST-GluA2-CT was added to the reaction solution and allowed for phosphorylation reaction by Src for 2 h. Then the reaction solution was boiled to inactivate Src. $CaCl_2$, $MgCl_2$, dithiothreitol and ATP (1.67 mM, 10 mM, 1 mM and 0.05 mM in final concentration, respectively) were added to the solution for the second phosphorylation reaction by PKC (Promega, Madison, WI) at 30°C for 2 h. The 2 × SDS-PAGE buffer was added and the samples were boiled.

Substrate Trap Assay. We prepared the catalytic domain of PTPMEG and its D820A mutant fused with the glutathione S-transferase (GST-PTP^{WT} and GST-PTP^{DA}, respectively) and quantified their protein content by BCA protein assay kit (Thermo Scientific). Eighteen hours after transfection of pCAGGS-GluA2 with Lipofectamine 2000 (Invitrogen), HEK293 cells were treated with the pervanadate solution composed of 145 NaCl, 5 KCl, 1 $CaCl_2$, 1 $MgCl_2$, 10 HEPES (pH 7.35), 1 H_2O_2 and 0.1 Na vanadate (in mM) for 30 min at 37°C. Cells were washed with phosphate-buffered saline (PBS) twice and were solubilized by the buffer containing 150 NaCl, 5 EDTA, 50 HEPES (pH 7.35), 50 NaF (in mM) and 1 % TritonX-100 supplemented with the

protease inhibitor cocktail (Calbiochem) at 4°C for 1 h. GST-fusion protein (4 μg) was added to the lysate and rotated at 4°C for 1 h. Then, the samples were incubated with glutathione sepharose beads (GE Healthcare, Little Chalfont, UK) at 4°C for additional 1 h with rotation to pull-down GST-protein. After 4 times wash with the solubilization buffer, 2 × SDS-PAGE buffer was applied and boiled for 5 min. Pulled-down proteins were subjected to western blot analysis using the antibodies against GluA2 (MilliPore), VCP, NSF (BD Biosciences, Franklin Lakes, NJ) and GST (GE Healthcare).

Mass Spectrometric Analysis. A synthetic phosphorylated GluA2 C-terminal peptide, pep-3pY (see *Electrophysiology*) was used as a substrate. GST-PTP^{WT}, its mutants (D820A, C852S) and GST were pre-bound to glutathione sepharose beads (GE Healthcare). Dephosphorylation reaction of pep-3pY (20 pmol) was performed for 30 min at 30°C in the buffer containing 25 mM HEPES (pH 7.35), 5 mM EDTA and 10 mM dithiothreitol by adding 2 μg of each GST-proteins. The reaction solution was boiled and centrifuged to remove the GST-proteins. GluA2 peptides in the supernatant was purified and concentrated using StageTips (Empore extraction disk; 3M, St. Paul, MN) and labeled with 4 iTRAQ reagents (Applied Biosystems/MDS Sciex, Foster City, CA) for 60 min at room temperature according to the manufacturer's instructions. iTRAQ-labeled GluA2 peptides were mixed and concentrated by vacuum evaporation and were subjected to mass spectrometric analysis using a 4800 MALDI-TOF-TOF Analyzer (Applied Biosystems/MDS). Mass spectral data were analyzed using the MASCOT program (Matrix Science) and the peaks derived from synthetic GluA2 peptides were identified. Peak areas for each iTRAQ signature were obtained by using ProteinPilot. For quantitative comparison, the data were normalized by the peak area of

GST–treated sample.

Biotinylation Assay. HEK293 cells transfected with pCAGGS-GluA2, -GluA2^{Y876F} or -GluA2^{Y869F,Y873F} were surface biotinylated using an ECL protein biotinylation kit (GE Healthcare). After stopping the biotinylation reaction, the cells were collected and solubilized with the buffer containing 150 NaCl, 50 Tris-HCl (pH 7.5), 5 EDTA (in mM), 1% NP-40 and the protease inhibitors (Calbiochem/Merck Biosciences) for 30 min at 4°C. The samples were centrifuged at 13,000 rpm for 15 min at 4°C. Streptavidin beads (Neutravidin agarose; Thermo Scientific) were added to the supernatant and incubated for 1 h at 4°C with rotation. Beads were washed 4 times with the solubilization buffer, boiled for 5 min, and subjected to the immunoblot analyses.

Immunohistochemisty. For immunohistochemical analysis, mice were fixed under deep anesthesia by cardiac perfusion with 0.1 M sodium phosphate buffer (PB), pH 7.4, containing 4% paraformaldehyde (4% PFA/PB); the cerebellum was then removed and soaked in 4% PFA/PB for 4 h. After rinsing the specimens with PBS, parasagittal slices (100 μm) were prepared using a microslicer (DTK-2000; Dosaka, Japan) and were permeabilized with 0.2% Triton X-100 in PBS with 2% normal goat serum and 2% bovine serum albumin for 6 h at 4°C. Immunohistochemical staining was performed using anti-mGluR1 (1:1,000; provided by Dr. M. Watanabe, Hokkaido University, Japan), anti-TRPC1 (1:200; Chemiccon) or anti-TRPC3 (1:200; Alomone lab) and anti-calbindin (1:10,000; Sigma) antibodies, followed by incubation with Alexa546 and Alexa488–conjugated secondary antibodies (1:1,000; Invitrogen), respectively. The stained slices were viewed using a confocal laser-scanning microscope (Fluoview;

Olympus).

Statistical Analysis. The results were described as means ± SEM. Statistical significance was defined as $P < 0.05$. When we compare the two groups, Mann-Whitney's *U* test was used. We performed Student *t*-test in the case of comparing the normalized values to the control (= 1). To compare multiple groups, one-way ANOVA followed by Bonferroni's *post hoc* tests was performed.

Acknowledgements. We thank Dr. R. L. Huganir and Dr. T. Hayashi for the anti-phosohoY876 GluA2 antibody, Dr. M. Watanabe for the anti-mGluR1α antibody and Dr. M. Mishina for the *GluD2*-null mouse. We also thank J. Motohashi and S. Narumi for their technical assistance. This work was supported by the Grant-in-Aid for the Ministry of Education, Culture, Sports, Science and Technology of Japan (K.K., W.K. and M.Y.), the CREST from the JST (M.Y.), the Keio Gijuku Academic Development Funds (K.K. and W.K.), the Keio University Medical Science Fund, Research Grants for Life Science and Medicine (K.K. and W.K.), the Naito Foundation (W.K.), the Inamori Foundation (W.K.), the PRESTO program from JST (S.M.), the Nakajima Foundation (W.K.), and the Takeda Science Foundation (W.K. and M.Y.).

References

1. Ito M (2002) The molecular organization of cerebellar long-term depression. *Nature reviews. Neuroscience* 3:896-902.

2. Kashiwabuchi N, et al. (1995) Impairment of motor coordination, Purkinje cell synapse formation, and cerebellar long-term depression in GluR delta 2 mutant mice. *Cell* 81:245-252.

3. Kohda K, et al. (2007) The extreme C-terminus of GluRdelta2 is essential for induction of long-term depression in cerebellar slices. *Eur J Neurosci* 25:1357-1362.

4. Kakegawa W, et al. (2008) Differential regulation of synaptic plasticity and cerebellar motor learning by the C-terminal PDZ-binding motif of GluRdelta2. *J Neurosci* 28:1460-1468.

5. Hirai H, et al. (2003) New role of delta2-glutamate receptors in AMPA receptor trafficking and cerebellar function. *Nat Neurosci* 6:869-876.

6. Man HY, et al. (2000) Regulation of AMPA receptor-mediated synaptic transmission by clathrin-dependent receptor internalization. *Neuron* 25:649-662.

7. Seidenman KJ, Steinberg JP, Huganir R, & Malinow R (2003) Glutamate receptor subunit 2 Serine 880 phosphorylation modulates synaptic transmission and mediates plasticity in CA1 pyramidal cells. *J Neurosci* 23:9220-9228.

8. Matsuda S, Launey T, Mikawa S, & Hirai H (2000) Disruption of AMPA receptor GluR2 clusters following long-term depression induction in cerebellar Purkinje neurons. *Embo J* 19:2765-2774.

9. Wang YT & Linden DJ (2000) Expression of cerebellar long-term depression requires postsynaptic clathrin-mediated endocytosis. *Neuron* 25:635-647.

10. Chung HJ, Steinberg JP, Huganir RL, & Linden DJ (2003) Requirement of AMPA receptor GluR2 phosphorylation for cerebellar long-term depression. *Science* 300:1751-1755.

11. Ahmadian G, et al. (2004) Tyrosine phosphorylation of GluR2 is required for insulin-stimulated AMPA receptor endocytosis and LTD. *Embo J* 23:1040-1050.

12. Moult PR, et al. (2006) Tyrosine phosphatases regulate AMPA receptor trafficking during metabotropic glutamate receptor-mediated long-term depression. *J Neurosci* 26:2544-2554.

13. Gladding CM, et al. (2009) Tyrosine dephosphorylation regulates AMPAR internalisation in mGluR-LTD. *Mol Cell Neurosci* 40:267-279.

14. Scholz R, et al. (2010) AMPA receptor signaling through BRAG2 and Arf6 critical for long-term synaptic depression. *Neuron* 66:768-780.

15. Hironaka K, Umemori H, Tezuka T, Mishina M, & Yamamoto T (2000) The

protein-tyrosine phosphatase PTPMEG interacts with glutamate receptor delta 2 and epsilon subunits. *J Biol Chem* 275:16167-16173.

16. Hayashi T & Huganir RL (2004) Tyrosine phosphorylation and regulation of the AMPA receptor by SRC family tyrosine kinases. *J Neurosci* 24:6152-6160.

17. Canepari M & Ogden D (2003) Evidence for protein tyrosine phosphatase, tyrosine kinase, and G-protein regulation of the parallel fiber metabotropic slow EPSC of rat cerebellar Purkinje neurons. *J Neurosci* 23:4066-4071.

18. Kim SJ, et al. (2003) Activation of the TRPC1 cation channel by metabotropic glutamate receptor mGluR1. *Nature* 426:285-291.

19. Hartmann J, et al. (2008) TRPC3 channels are required for synaptic transmission and motor coordination. *Neuron* 59:392-398.

20. Jeromin A, Huganir RL, & Linden DJ (1996) Suppression of the glutamate receptor delta 2 subunit produces a specific impairment in cerebellar long-term depression. *Journal of neurophysiology* 76:3578-3583.

21. Tanaka K & Augustine GJ (2008) A positive feedback signal transduction loop determines timing of cerebellar long-term depression. *Neuron* 59:608-620.

22. Huang CC & Hsu KS (2006) Sustained activation of metabotropic glutamate receptor 5 and protein tyrosine phosphatases mediate the expression of (S)-3,5-dihydroxyphenylglycine-induced long-term depression in the hippocampal CA1 region. *J Neurochem* 96:179-194.

23. Yu SY, Wu DC, Liu L, Ge Y, & Wang YT (2008) Role of AMPA receptor trafficking in NMDA receptor-dependent synaptic plasticity in the rat lateral amygdala. *J Neurochem* 106:889-899.

24. Brebner K, et al. (2005) Nucleus accumbens long-term depression and the expression of behavioral sensitization. *Science* 310:1340-1343.

25. Kina S, et al. (2007) Involvement of protein-tyrosine phosphatase PTPMEG in motor learning and cerebellar long-term depression. *Eur J Neurosci* 26:2269-2278.

26. Tiganis T & Bennett AM (2007) Protein tyrosine phosphatase function: the substrate perspective. *Biochem J* 402:1-15.

27. Zhang SH, Liu J, Kobayashi R, & Tonks NK (1999) Identification of the cell cycle regulator VCP (p97/CDC48) as a substrate of the band 4.1-related protein-tyrosine phosphatase PTPH1. *J Biol Chem* 274:17806-17812.

28. Yuzaki M (2012) Cerebellar LTD vs. motor learning-Lessons learned from studying GluD2. *Neural networks : the official journal of the International Neural Network Society.*

29. Boxall AR, Lancaster B, & Garthwaite J (1996) Tyrosine kinase is required for long-term depression in the cerebellum. *Neuron* 16:805-813.

30. Hartell NA (2001) Receptors, second messengers and protein kinases required for heterosynaptic cerebellar long-term depression. *Neuropharmacology* 40:148-161.

31. Tsuruno S, Kawaguchi SY, & Hirano T (2008) Src-family protein tyrosine kinase negatively regulates cerebellar long-term depression. *Neurosci Res* 61:329-332.

32. Luscher C & Huber KM (2010) Group 1 mGluR-dependent synaptic long-term depression: mechanisms and implications for circuitry and disease. *Neuron* 65:445-459.

33. Gladding CM, Fitzjohn SM, & Molnar E (2009) Metabotropic glutamate receptor-mediated long-term depression: molecular mechanisms. *Pharmacological reviews* 61:395-412.

34. Liu YF, et al. (2004) Serine phosphorylation proximal to its phosphotyrosine binding domain inhibits insulin receptor substrate 1 function and promotes insulin resistance. *Mol Cell Biol* 24:9668-9681.

35. Sanz-Clemente A, Matta JA, Isaac JT, & Roche KW (2010) Casein kinase 2 regulates the NR2 subunit composition of synaptic NMDA receptors. *Neuron* 67:984-996.

36. Unoki T, et al. (2012) NMDA receptor-mediated PIP5K activation to produce PI(4,5)P is essential for AMPA receptor endocytosis during LTD. *Neuron* 73:135-148.

37. Lomeli H, et al. (1993) The rat delta-1 and delta-2 subunits extend the excitatory amino acid receptor family. *FEBS letters* 315:318-322.

38. Kim CH, Chung HJ, Lee HK, & Huganir RL (2001) Interaction of the AMPA receptor subunit GluR2/3 with PDZ domains regulates hippocampal long-term depression. *Proc Natl Acad Sci U S A* 98:11725-11730.

39. Takeuchi T, et al. (2008) Enhancement of both long-term depression induction and optokinetic response adaptation in mice lacking delphilin. *PLoS One* 3:e2297.

40. Miyagi Y, et al. (2002) Delphilin: a novel PDZ and formin homology domain-containing protein that synaptically colocalizes and interacts with glutamate receptor delta 2 subunit. *J Neurosci* 22:803-814.

41. Zhang Y, et al. (2008) The tyrosine phosphatase STEP mediates AMPA receptor endocytosis after metabotropic glutamate receptor stimulation. *J Neurosci* 28:10561-10566.

42. Lombroso PJ, Murdoch G, & Lerner M (1991) Molecular characterization of a protein-tyrosine-phosphatase enriched in striatum. *Proc Natl Acad Sci U S A* 88:7242-7246.

43. Young JA, et al. (2008) The protein tyrosine phosphatase PTPN4/PTP-MEG1, an enzyme capable of dephosphorylating the TCR ITAMs and regulating NF-kappaB, is dispensable for T cell development and/or T cell effector functions. *Mol Immunol* 45:3756-3766.

44. Linden DJ (1996) A protein synthesis-dependent late phase of cerebellar long-term depression. *Neuron* 17:483-490.

45. Gu M & Majerus PW (1996) The properties of the protein tyrosine phosphatase PTPMEG. *J Biol Chem* 271:27751-27759.

46. Coles CH, et al. (2011) Proteoglycan-specific molecular switch for RPTPsigma clustering and neuronal extension. *Science* 332:484-488.

47. Matsuda K, et al. (2010) Cbln1 is a ligand for an orphan glutamate receptor delta2, a bidirectional synapse organizer. *Science* 328:363-368.

48. Kakegawa W, et al. (2011) D-serine regulates cerebellar LTD and motor coordination through the delta2 glutamate receptor. *Nat Neurosci* 14:603-611.

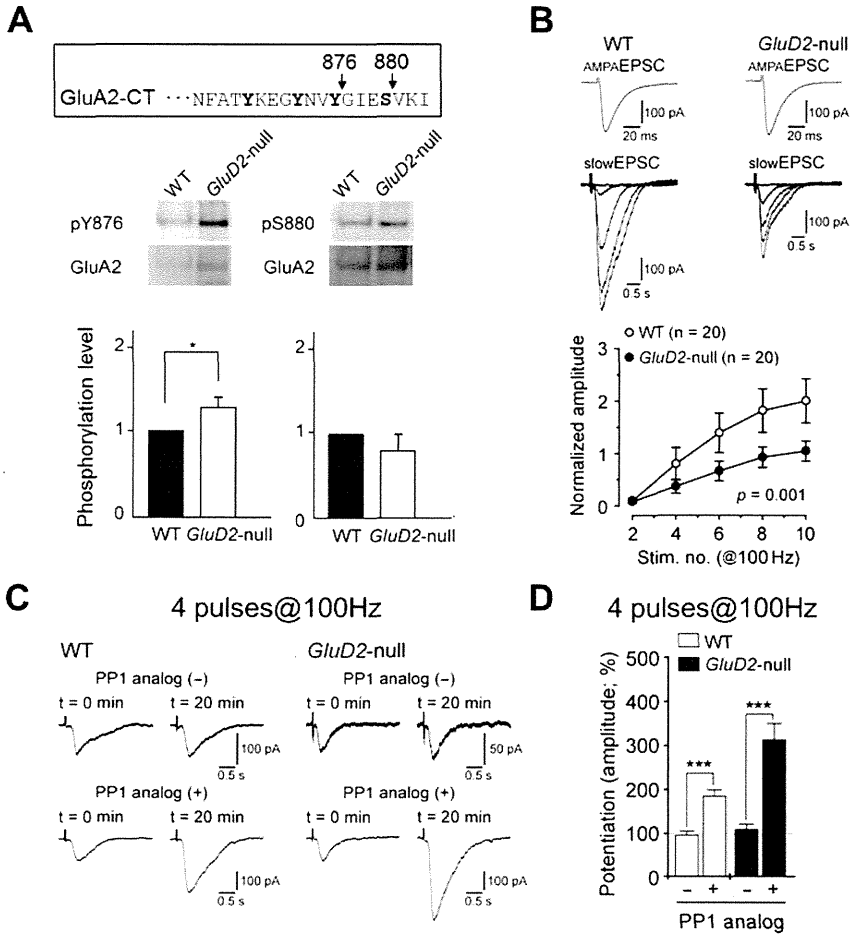

Fig. 1. Increased tyrosine phosphorylation in *GluD2*-null mice. (*A*) Basal-state phosphorylation of Y876 and S880 of GluA2 subunits of AMPA receptors in *GluD2*-null mice. The upper schema illustrates positions of Y876 and S880 at the C terminus of GluA2 (GluA2-CT). Representative immunoblot images of the synaptosomal fraction of WT and *GluD2*-null cerebellum using an antibody against phosphorylated Y876 (pY876) or S880 (pS880) are shown in the middle panel. The lower graph shows intensities of pY876 bands (*Left*) or pS880 bands (*Right*) in *GluD2*-null cerebellum normalized by those in WT cerebellum. Basal-state phosphorylation of Y876, but not S880, was significantly increased in *GluD2*-null than in WT cerebellum. The bar represents mean and SEM. * denotes $P < 0.05$. n = 11 for Y876, n = 7 for S880. (*B*) Reduced $_{slow}$EPSC amplitudes in *GluD2*-null Purkinje cells. By adjusting PF stimulus intensities, similar sizes of PF–evoked $_{AMPA}$EPSCs were obtained in *GluD2*-null and WT Purkinje cells (*Upper*). Then PFs were stimulated for 2 to 10 times at 100 Hz in the presence of AMPA receptor blockers to evoke $_{slow}$EPSCs (*Lower*). Amplitudes of $_{slow}$EPSCs were normalized by those of $_{AMPA}$EPSCs and plotted against the number of stimulations in the lower graphs. The bar represents mean and SEM. $P = 0.001$. n = 20 each. (*C, D*) $_{slow}$EPSC amplitudes are enhanced by a SFK inhibitor PP1 analog in both WT and *GluD2*-null Purkinje cells. PFs were stimulated for 4 times at 100 Hz in the presence of AMPA receptor blockers to evoke $_{slow}$EPSCs. When a PP1 analog was not included in the patch pipette [PP1 analog (–), upper traces], there were no changes in amplitudes of $_{slow}$EPSCs just after breaking into whole-cell mode and 20 min later, whereas when a PP1 analog was included [(+), lower traces], amplitudes of $_{slow}$EPSCs at 20 min were significantly increased in both WT and *GluD2*-null Purkinje cells. The bar graph shows potentiating effects by a PP1 analog on $_{slow}$EPSCs, which were normalized by those of $_{AMPA}$EPSCs, in WT and *GluD2*-null Purkinje cells (*D*). The bar represents mean and SEM. *** denotes $P < 0.005$. n = 11 for each group.

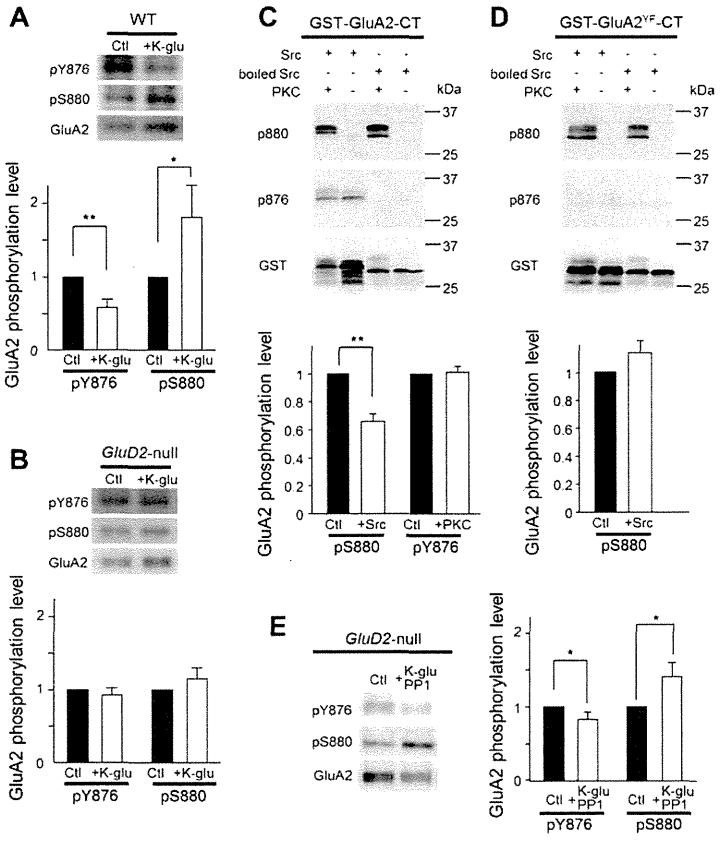

Fig. 2. Increased Y876 phosphorylation inhibits S880 phosphorylation. (*A, B*) Chemical LTD stimulus decreases Y876 phosphorylation but increases S880 phosphorylation in WT cerebellum (*A*), whereas it induces no changes at both sites in *GluD2*-null cerebellum (*B*). WT and *GluD2*-null cerebellar slices were treated with 50 mM KCl plus 10 μM L-glutamate for 5 min (K-glu) and the cell lysates were subjected to immunoblot analyses using phosphorylation-specific antibodies against Y876 (pY876) and S880 (pS880). Representative immunoblot images are shown on top panels. In the lower graphs, intensities of pY876 and pS880 bands in K-glu–treated slices were normalized to those in untreated slices. The bar represents mean and SEM. * and ** denote $P < 0.05$ and $P < 0.01$, respectively. n = 8 each for WT and n = 13 each for *GluD2*-null cerebellum. (*C, D*) Y876 phosphorylation inhibits subsequent S880 phosphorylation in the *in vitro* phosphorylation assay. The C-terminal region of GluA2 was conjugated with GST (GST-GluA2-CT). Y876 was replaced with phenylalanine to produce GST-GluA2^{YF}-CT. GST-GluA2-CT (*C*) or GST-GluA2^{Y876F}-CT (*D*) was incubated with Src or boiled Src, followed by PKC. Phosphorylation of GluA2 was detected by anti-phospho-Y876 and -S880 specific antibodies. Representative immunoblot images are shown in the top panels. The diagrams show intensities of S880 phosphorylation levels (pS880) with prior Src treatment (+Src) normalized by those with boiled Src (Ctl). Intensities of Y876 phosphorylation levels (pY876) with subsequent PKC treatment (+PKC) normalized by those without Src (Ctl) are also shown. The bar represents mean and SEM. ** denotes $P < 0.01$. n = 11 for pY876 and n = 13 for pS880. (*E*) Inhibition of tyrosine phosphorylation restores K-glu–evoked changes in Y876 and S880 phosphorylation in *GluD2*-null cerebellum. Cerebellar slices from *GluD2*-null mice were incubated with a PP1 analog for 15 min and then treated with K-glu in the presence of a PP1 analog. K-glu treatment significantly decreased Y876 phosphorylation and increased S880 phosphorylation in *GluD2*-null cerebellum. Representative immunoblot images are shown in the left panels. In the right diagram, intensities of pY876 and pS880 bands in K-glu–treated slices were normalized to those in untreated slices. The bar represents mean and SEM. * denotes $P < 0.05$. n = 16 for pY876 and n = 17 for pS880.

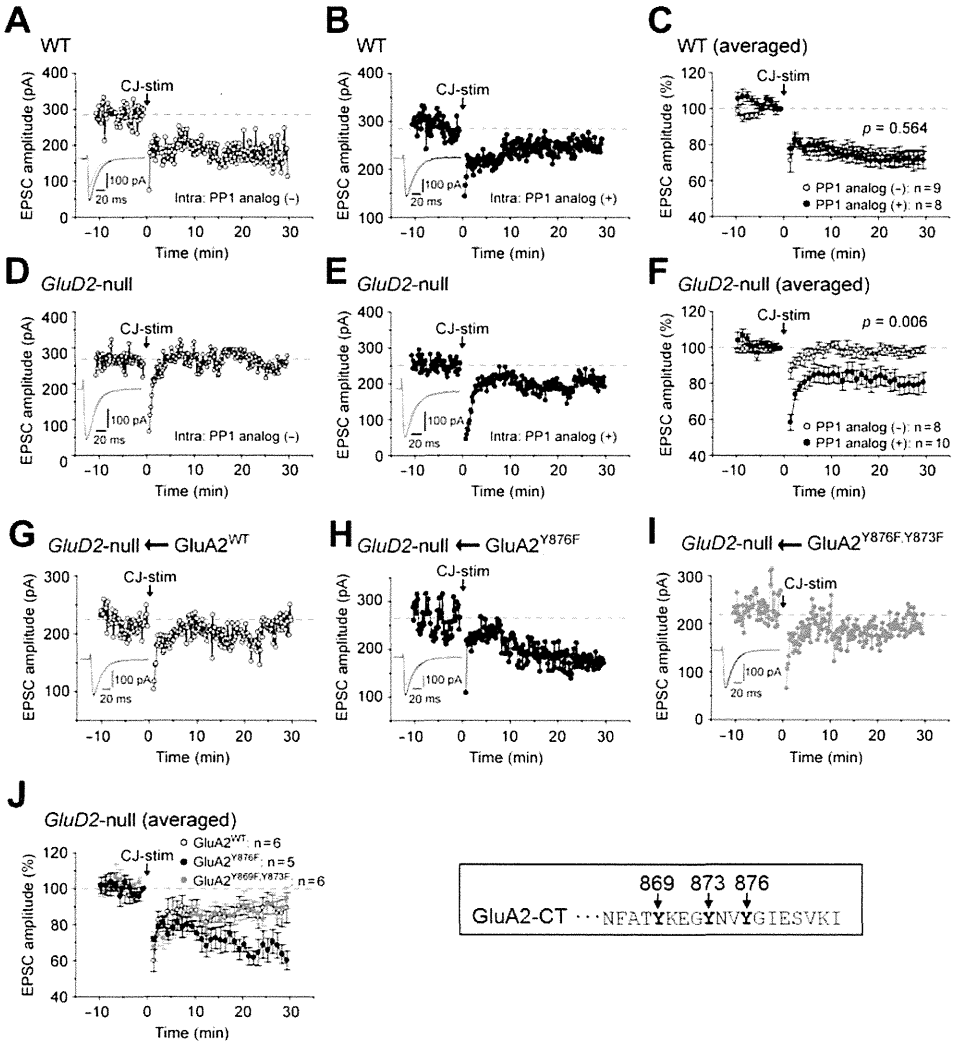

Fig. 3. Dephosphorylation of tyrosine of GluA2 is sufficient to restore LTD induction in *GluD2*-null Purkinje cells. (*A–F*) Inclusion of a PP1 analog in a patch pipette restored LTD in *GluD2*-null Purkinje cells but it did not affect LTD in WT Purkinje cells. Application of CJ-stim (consisting of 30 cycles of PF stimulation plus Purkinje cell depolarization at 1 Hz) induced LTD in WT Purkinje cells with (+) or without (–) a PP1 analog (10 μM) in patch pipettes (*A*, *B*). CJ-stim successfully induced LTD in *GluD2*-null Purkinje cells with (+; *E*), but not those without (–; *D*) a PP1 analog. Collective results (mean and SEM) are shown in (*C*, *F*). The inset sweeps show PF–EPSCs just before (black traces) and 30 min after (gray traces) CJ-stim. (*G–J*) Overexpression of unphosphorable GluA2 subunits restored LTD induction in *GluD2*-null Purkinje cells. Y869, Y873, and Y876 phosphorylation sites (shown in the right of *J*) were replaced with phenylalanine to produce unphosphorable GluA2 mutants termed as $GluA2^{Y876F}$ and $GluA2^{Y869F,Y873F}$. $GluA2^{WT}$, $GluA2^{Y876F}$, and $GluA2^{Y869F,Y873F}$ were overexpressed in *GluD2*-null Purkinje cells by a Sindbis virus vector. CJ-stim–induced LTD was restored in *GluD2*-null Purkinje cells expressing $GluA2^{Y876F}$ (*H*), but not those expressing $GluA2^{WT}$ (*G*) or $GluA2^{Y869F,Y873F}$ (*I*). Collective data (mean and SEM) are shown in (*J*). The inset sweeps show PF–EPSCs just before (black traces) and 30 min after (gray traces) CJ-stim.

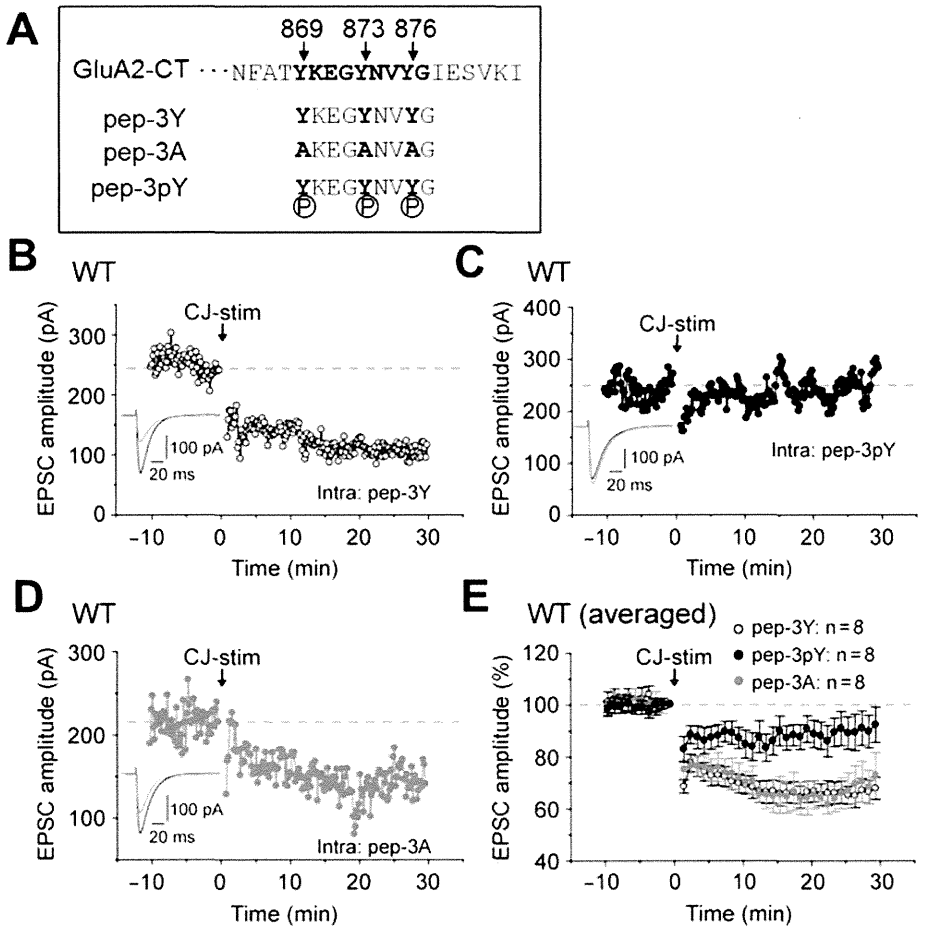

Fig. 4. Dephosphorylation of tyrosine of GluA2 is necessary for LTD induction in WT Purkinje cells. (*A*) Diagram indicating three peptides used in this study. Synthetic peptides correspond to the GluA2 C terminus between position 869 and 877. Alanine replaced three tyrosine residues in the original peptide (pep-3Y) to produce unphosphorable peptide (pep-3A). All tyrosine residues were phosphorylated in pep-3pY. (*B-E*) LTD is specifically inhibited by pep-3pY, which could serve as a pseudosubstrate for tyrosine phosphatase, included in Purkinje cells. Inclusion of pep-3Y (*B*) or pep-3A (*D*) in patch pipettes did not affect CJ-stim–induced LTD in WT Purkinje cells, but pep-3pY (*C*) inhibited LTD induction. Collective data (mean and SEM) are shown in (*E*). The inset sweeps show PF–EPSCs before and 30 min after CJ-stim.

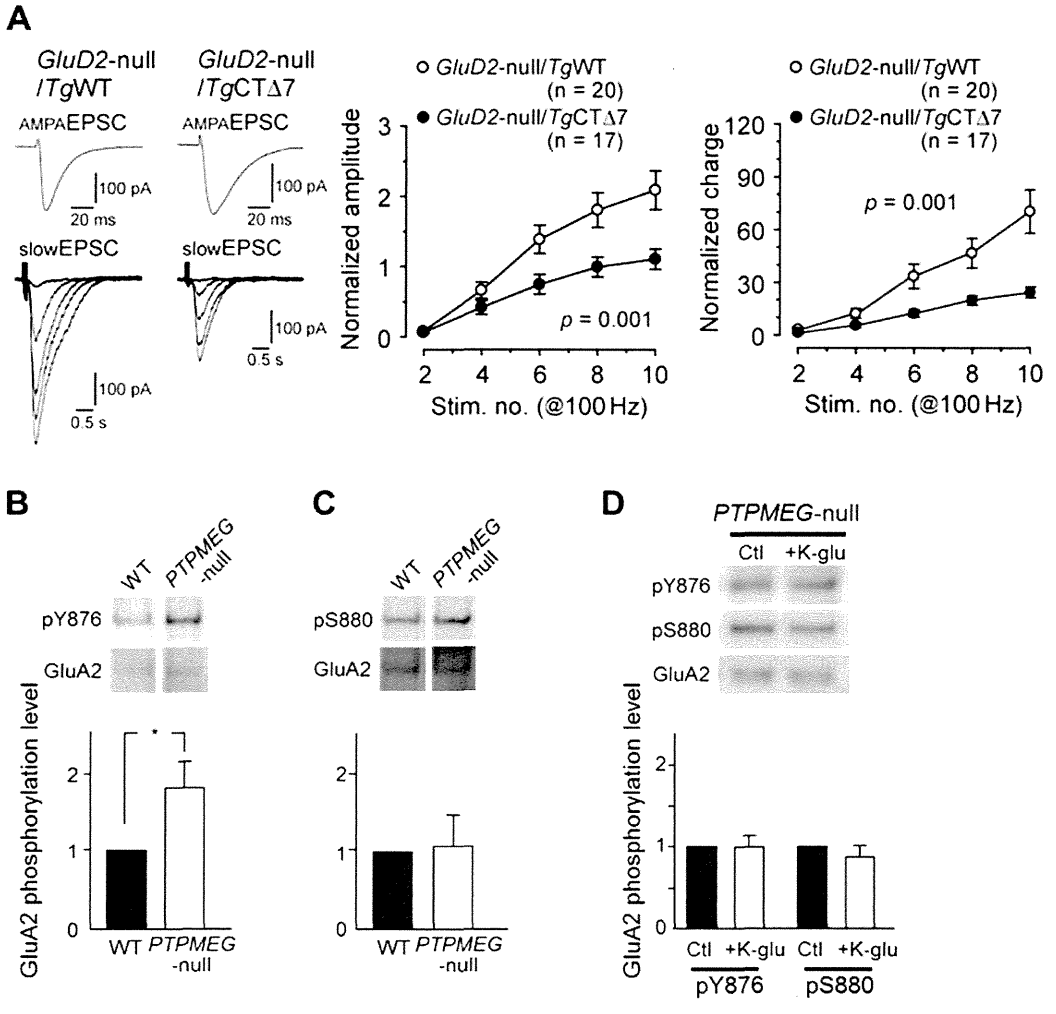

Fig. 5. PTPMEG regulates tyrosine dephosphorylation levels at PF–Purkinje cell synapses. (*A*) Seven C-terminal amino acids of GluD2 determine $_{slow}$EPSC amplitudes in Purkinje cells. $_{slow}$EPSCs were evoked in *GluD2*-null Purkinje cells expressing WT GluD2 transgenes (*GluD2*-null/*Tg*WT) or mutant GluD2 transgenes lacking the seven C-terminal amino acids (*GluD2*-null/*Tg*CTΔ7) as described in the legend of **Fig. 1C**. Representative traces are shown in the left panel. Amplitudes and charges of $_{slow}$EPSCs were normalized by those of $_{AMPA}$EPSCs and plotted against the number of stimulations in the right graphs. The bar represents mean and SEM. (*B*, *C*) Basal phosphorylation of Y876 and S880 of GluA2 subunits in *PTPMEG*-null mice. Representative immunoblot images of the synaptosomal fraction of WT and *PTPMEG*-null cerebellum using an antibody against pY876 or pS880 are shown in the top panel. The lower graph shows intensities of pY876 bands (*B*) or pS880 bands (*C*) in *PTPMEG*-null cerebellum normalized by those in WT cerebellum. Basal phosphorylation of Y876, but not of S880, was significantly increased in *PTPMEG*-null than in WT cerebellum. The bar represents mean and SEM. * denotes $P < 0.05$. n = 10 for Y876, n = 7 for S880. (*D*) Chemical LTD stimulus induces no changes at Y876 and S880 sites in *PTPMEG*-null cerebellum. *PTPMEG*-null cerebellar slices were treated with 50 mM KCl plus 10 μM L-glutamate for 5 min (K-glu) and the cell lysates were subjected to immunoblot analyses using phosphorylation-specific antibodies against pY876 and pS880. Representative immunoblot images are shown in the top panels. In the lower graphs, intensities of pY876 and pS880 bands in K-glu–treated slices were normalized to those in untreated slices. The bar represents mean and SEM. n = 15 each.

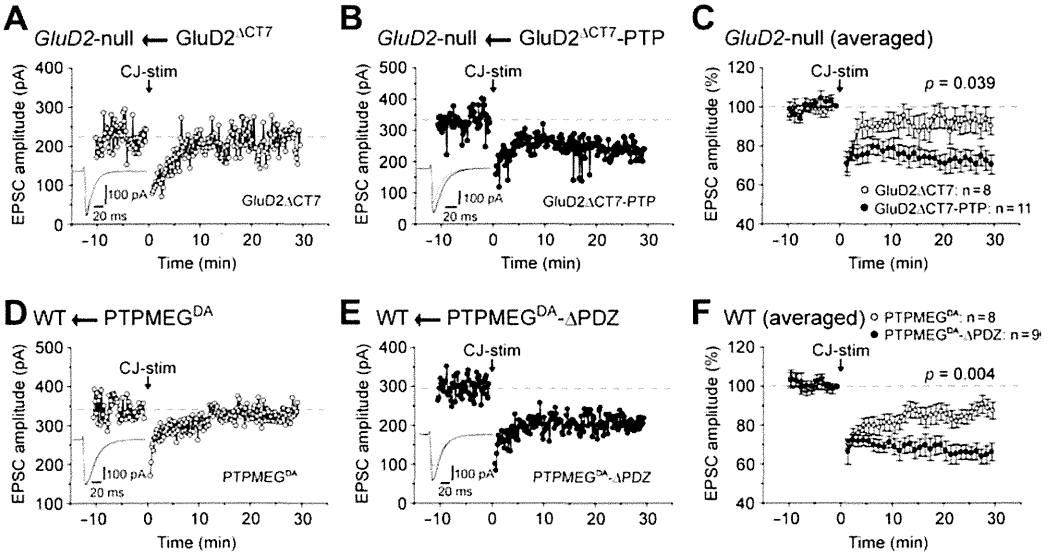

Fig. 6. Interaction of GluD2 with enzymatically active PTPMEG is necessary for LTD induction. (*A–C*) The catalytic domain of PTPMEG was sufficient to restore LTD in *GluD2*-null mice. The catalytic phosphatase domain of PTPMEG was directly fused to the C terminus of a mutant GluD2 lacking the seven C-terminal amino acids (GluD2$^{\Delta CT7}$) to produce GluD2$^{\Delta CT7}$-PTP. GluD2$^{\Delta CT7}$ and GluD2$^{\Delta CT7}$-PTP were expressed in *GluD2*-null Purkinje cells by the Sindbis virus vector. CJ-stim induced LTD in *GluD2*-null Purkinje cells expressing GluD2$^{\Delta CT7}$-PTP (*B*), but not in those expressing GluD2$^{\Delta CT7}$ (*A*). Collective data (mean and SEM) are shown in (*C*). The inset sweeps show PF–EPSCs just before (black traces) and 30 min after (gray traces) CJ-stim. (*D–F*) Interaction with endogenous PTPMEG is necessary for LTD in WT Purkinje cells. A substrate-trapping mutant PTPMEG (PTPMEG^{DA}) was produced by replacing aspartate in the catalytic domain with alanine. The PDZ domain, by which PTPMEG binds to the C terminus of GluD2, was further deleted to produce PTPMEG^{DA}-ΔPDZ. PTPMEG^{DA} or PTPMEG^{DA}-ΔPDZ was transduced into WT Purkinje cells using a Sindbis virus vector. CJ-stim–evoked LTD was inhibited in Purkinje cells expressing PTPMEG^{DA} (*D*) but not in those expressing PTPMEG^{DA}-ΔPDZ (*E*), indicating that PTPMEG^{DA} bound to GluD2 and replaced endogenous PTPMEG as a dominant-negative molecule. Collective data (mean and SEM) are shown in (*F*). The inset sweeps show PF–EPSCs just before (black traces) and 30 min after (gray traces) CJ-stim.

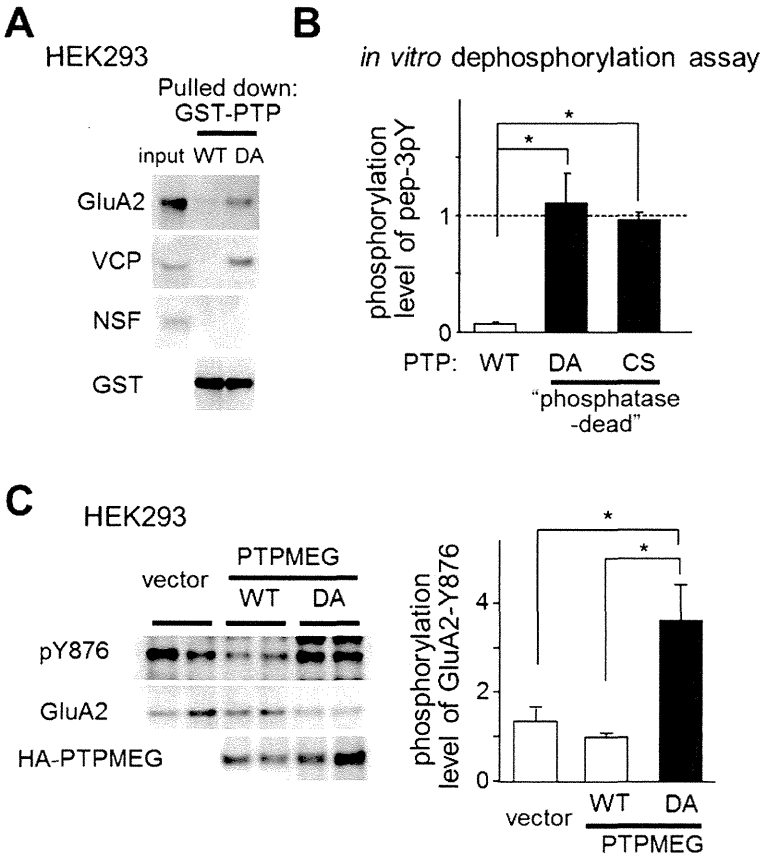

Fig. 7. GluA2 is a substrate of PTPMEG. (*A*) A substrate-trap mutant of PTPMEG interacts with GluA2. The cell lysate of HEK293 cells transfected with GluA2 was pulled down with the catalytic domain of PTPMEG fused with GST (GST-PTP). Aspartate in the catalytic center was replaced with alanine to produce a substrate-trap mutant (GST-PTP^{DA}). As reported for a related phosphatase PTPH1, endogenous VCP was trapped by GST-PTP^{DA}, but not by GST-PTP. NSF, a protein related to VCP, was not pulled down by GST-PTP^{DA} or GST-PTP. Similarly, GluA2 was more effectively pulled down by GST-PTP^{DA}. (*B*) GluA2 C-terminal peptides are directly dephosphorylated by PTPMEG *in vitro*. Cysteine in the catalytic center was replaced with serine to produce another substrate trap mutant (GST-PTP^{CS}). A tyrosine-phosphorylated synthetic peptide, pep-3pY, derived from the C terminus (869–877) of GluA2 was incubated with GST-PTP, GST-PTP^{DA}, GST-PTP^{CS}, or GST alone and subjected to the isobaric tag-based quantitative mass spectrometric analyses. The diagram indicates phosphorylation levels of peptides treated with each GST-fusion protein normalized by those treated with GST alone. Bars represent mean and SEM. * denotes $P < 0.05$. n = 6 for each group. (*C*) PTPMEG dephosphorylates Y876 of GluA2 in HEK293 cells. GluA2 and WT or a phosphatase-inactive mutant (DA) PTPMEG were coexpressed in HEK293 cells and the cell lysates were subjected to immunoblot analyses using a phosphorylation-specific antibody against pY876. Representative immunoblot images are shown in the left panel. The right diagram shows intensities of pY876 bands normalized by those in cells expressing WT PTPMEG. Phosphorylation levels of Y876 of GluA2 were significantly higher in cells coexpressing a phosphatase-inactive mutant PTPMEG. The bar represents mean and SEM. * denotes $P < 0.05$. n = 8 for each group.

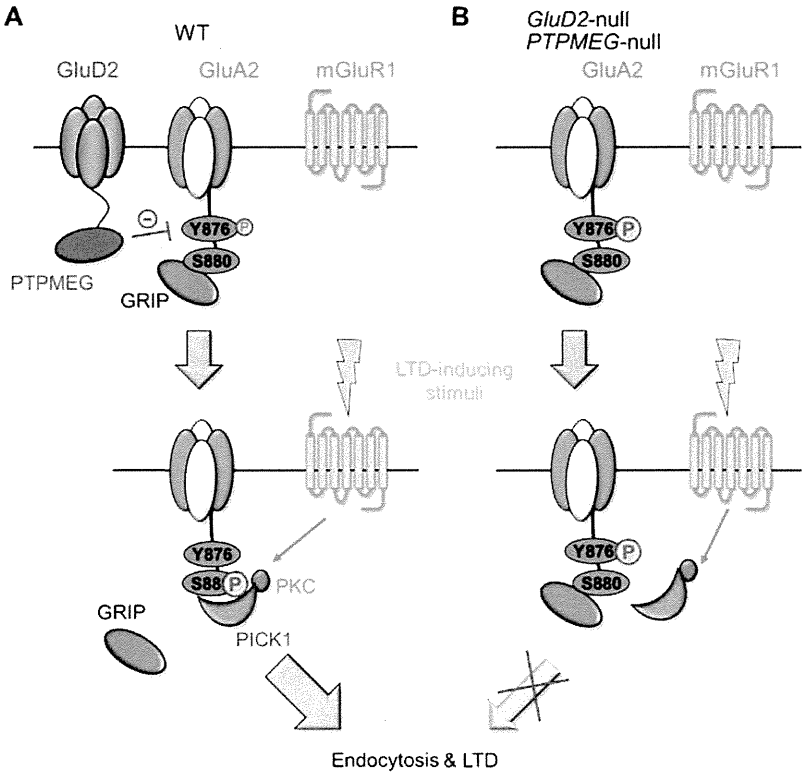

Fig. 8. A proposed role of GluD2 in the regulation of "inducibility" of cerebellar LTD. (*A*) In WT cerebellum, GluD2 maintains low levels of phosphorylation at Y876 of the GluA2 subunit of AMPA receptors via PTPMEG that binds to the C-terminus. LTD-inducing stimuli further dephosphorylates Y876 by unknown mechanisms, including activation of PTPMEG by conformational changes of GluD2 and inactivation of SFKs. Y876 dephosphorylation allows S880 phosphorylation by protein kinase C (PKC), leading to the replacement of anchoring proteins from GRIP to PICK1 and allowing AMPA receptor endocytosis during LTD. (*B*) In *GluD2*-null and *PTPMEG*-null Purkinje cells, high basal-state phosphorylation at Y876 prevents subsequent phosphorylation at S880 of GluA2 during LTD–inducing stimulus, thus inhibits GluA2 endocytosis and LTD.

Supporting Information

Kohda et al.
Gating of LTD by δ2 glutamate receptors–a new mechanism by coordinated interaction between two AMPA receptor phosphorylation sites

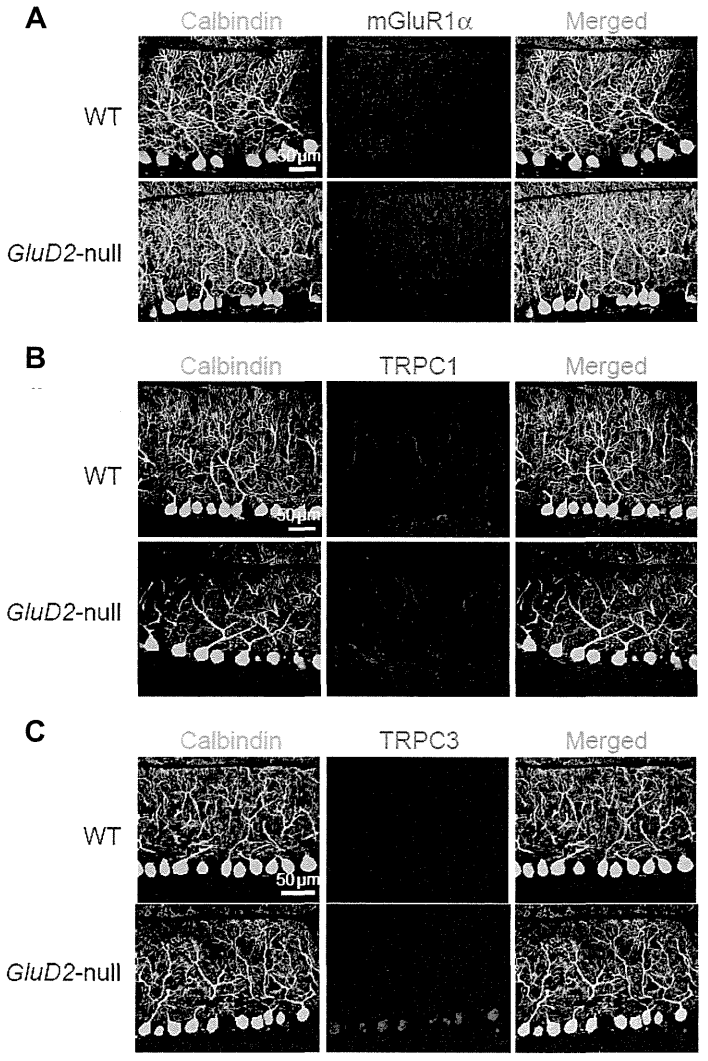

Fig. S1. Expression patterns of molecules involved in $_{slow}$EPSCs do not change in *GluD2*-null cerebellum. (*A–C*) Cerebellar slices from wild-type (WT) or *GluD2*-null mice were immunostained with mGluR1α (*A*), TRPC1 (*B*) and TRPC3 (*C*). Purkinje cells were coimmunostained with its marker, calbindin (green).

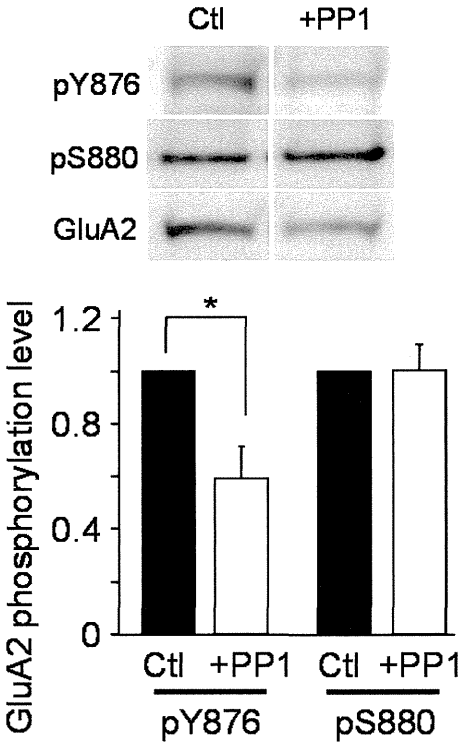

Fig. S2. Incubation with a SFK inhibitor decreases basal-state Y876 phosphorylation levels without changing S880 phosphorylation levels in *GluD2*-null cerebellum. Cerebellar slices from *GluD2*-null mice were incubated with a PP1 analog for 15 min and subjected to immunoblot analyses using phosphorylation–specific antibodies against pY876 and pS880. Representative immunoblot images are shown on top panels. In the lower diagram, intensities of pY876 and pS880 bands in PP1–treated slices were normalized to those in untreated slices. The bar represents mean and SEM. * denotes $P < 0.05$. n = 3 each.

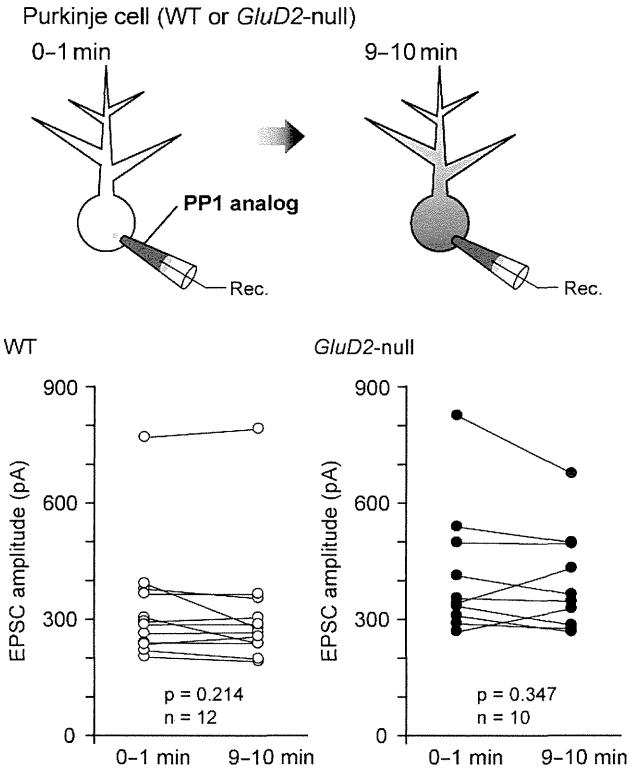

Fig. S3. Application of a SFK inhibitor does not change PF–EPSC amplitudes in wild-type (WT) and *GluD2*-null Purkinje cells. When a PP1 analog was included in the patch pipette, there were no changes in amplitudes of PF–EPSCs just after breaking into whole-cell mode and 10 min later.